

# A Novel Pilot Allocation Technique for Uplink OFDMA in ISAC Systems

Ahmet Sacid Sümer, Ebubekir Memişoğlu and Hüseyin Arslan, *Fellow, IEEE*,

**Abstract**—In integrated sensing and communication (ISAC) systems, pilot signals play a crucial role in enhancing sensing performance due to their strong autocorrelation properties and high transmission power. However, conventional interleaved pilots inherently constrain the maximum unambiguous range and reduce the accuracy of channel impulse response (CIR) estimation compared to continuous orthogonal frequency-division multiple access (OFDMA) signals. To address this challenge, we propose a novel overlapped block-pilot structure for uplink OFDMA-based ISAC systems, called phase-shifted ISAC (PS-ISAC) pilot allocation. The proposed method leverages a cyclic prefix (CP)-based phase-shifted pilot design, enabling efficient multi-transmitter pilot separation at the receiver. Simulation results confirm that the proposed scheme enhances CIR separation, reduces computational complexity, and improves mean square error (MSE) performance under practical power constraints. Furthermore, we demonstrate that utilizing continuous pilot resources maximizes the unambiguous range.

**Index Terms**—Integrated sensing and communication (ISAC), channel impulse response (CIR), orthogonal frequency-division multiple access (OFDMA), pilot design, uplink (UL).

## I. INTRODUCTION

INTEGRATED sensing and communication (ISAC) has garnered significant attention from academia and industry due to its potential to enhance spectral, energy, and hardware efficiency by sharing spectrum and hardware resources for both sensing and communication functions [1]. A key challenge in ISAC is designing multiple access (MA) techniques that balance communication and sensing while minimizing mutual interference [2], [3]. In this context, next-generation MA (NGMA) techniques are expected to play a crucial role in 6G wireless networks by optimizing resource allocation for dual functionality. From a resource allocation perspective, MA techniques must balance the trade-off between sensing and communication [4]. However, conventional MA approaches, designed primarily for communication, may not be directly applicable to ISAC due to their inherent constraints in pilot allocation, interference management, and coexistence strategies.

In ISAC, pilot allocation plays a pivotal role in balancing the coexistence of sensing and communication signals. Traditionally, pilots have been employed in communication for channel estimation and positioning [5], while also serving as essential components in sensing applications [6]. Given this

dual functionality, different wireless standards have adopted distinct pilot allocation strategies to optimize performance. Recognizing this, Wi-Fi integrates sensing by transmitting pilot-only packets, utilizing the same channel access mechanisms as communication packets [7]. Meanwhile, in OFDMA-based systems, pilot allocation follows a structured approach, broadly classified into two categories: block and interleaved pilot allocation [8]. A promising approach is uplink (UL) overlapped interleaved pilot allocation, where time-shifted pilot sequences are leveraged to separate the channel impulse responses (CIRs) of multiple transmitters in the time domain [9]. Additionally, to mitigate excessive pilot overhead, overlapping pilots have been explored in prior studies [10], where Kalman estimators and predictive filtering techniques have been used to enhance the channel estimation process in UL overlapped interleaved allocation. However, these methods do not account for the unique requirements of ISAC, such as a high maximum unambiguous range and velocity estimation.

**ISAC pilot designs:** In orthogonal frequency-division multiple access (OFDMA) systems, pilot signals are typically non-continuous and uniformly interleaved across the time and frequency domains. Beyond communication, these structured pilots have also been explored for sensing applications. Radar processing techniques leveraging pilots in the orthogonal frequency-division multiplexing (OFDM) waveform, along with dynamic pilot subcarrier allocation for range-adaptive radar sensing, have been investigated in the downlink (DL) [11], [12]. Additionally, the potential use of 5G positioning reference signals (PRS) for radar sensing in the DL has been explored in [6]. However, conventional pilot allocation schemes, originally designed for communication, suffer from reduced resolution and limited unambiguous range due to their interleaved spectrum occupation. To address this limitation, a coprime and periodic pilot design was proposed in [13] as an interleaved pilot allocation strategy for the DL. While this approach enhances the maximum unambiguous range, it introduces additional computational complexity. Furthermore, in the UL, ISAC-oriented pilot allocation techniques have been investigated in the context of overlapped pilot and sensing sequences [14], [15]. These methods primarily rely on interleaved pilot structures and iterative channel estimation, demonstrating effectiveness in sensing but also increasing computational complexity.

Despite the growing interest in ISAC pilot allocation, there remains a lack of research on block pilot structures in an overlapped manner for UL OFDMA-based ISAC systems. Current interleaved methods suffer from low pilot density, which degrades channel estimation accuracy and restricts the maximum

The authors are with the Department of Electrical and Electronics Engineering, Istanbul Medipol University, Istanbul, 34810, Turkey (e-mail: ahmet.sumer@std.medipol.edu.tr; ememisoglu@medipol.edu.tr; huseyinarslan@medipol.edu.tr).

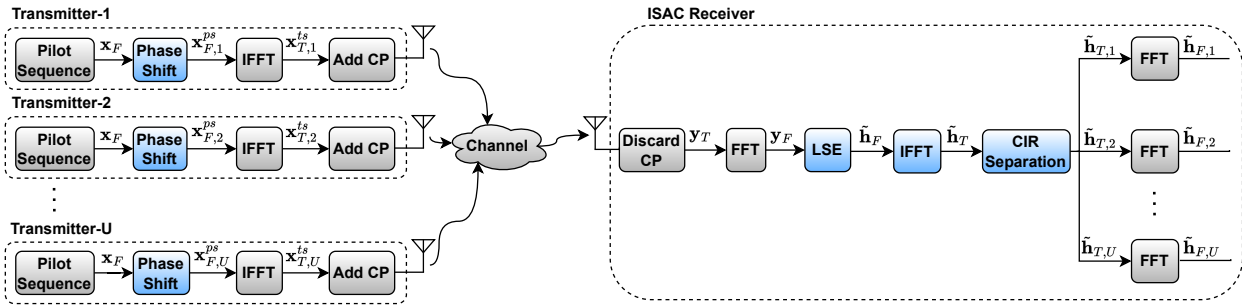


Fig. 1. The system model of the proposed uplink ISAC multiple-access scheme.

unambiguous range. Therefore, there is a pressing need for a novel MA strategy for UL pilot allocation that overcomes these challenges without introducing excessive complexity. Such a solution must maximize the unambiguous range limit, enhance sensing accuracy, minimize computational overhead, and ensure robust multi-transmitter CIR separation in overlapped pilot allocation schemes for OFDMA-based ISAC systems.

**Contributions of this work:** In this work, we propose a novel overlapped block-pilot structure for UL OFDMA-based ISAC systems, introducing a cyclic prefix (CP)-based phase-shifted pilot allocation to enable efficient multi-transmitter pilot separation at the receiver. The proposed phase-shifted-ISAC (PS-ISAC) method ensures continuous pilot transmission, effectively enhancing the maximum unambiguous range while optimizing spectral utilization. Performance evaluation confirms that PS-ISAC outperforms conventional interleaved pilot allocation—widely used in standardized OFDMA systems [16]—by achieving lower mean-square error (MSE) under power spectral constraints with reduced computational complexity. These results establish the overlapped block-pilot structure as a robust and efficient alternative to standardized orthogonal interleaved schemes, offering enhanced estimation accuracy and resource utilization for ISAC systems.

## II. SYSTEM MODEL

The proposed system model, illustrated in Fig. 1<sup>1</sup>, consists of  $U$  single-antenna transmitters, each functioning as either a communication or sensing transmitter in an UL OFDMA transmission. These transmitters simultaneously transmit their signals over a channel to a single-antenna ISAC receiver, sharing the same time and frequency resources to maximize spectrum efficiency. Each OFDM symbol is structured based on the transmitter type: communication transmitters use pilot carriers, while sensing transmitters use dedicated sequences<sup>2</sup>. During transmission, pilots  $x_F$ <sup>3</sup> are inserted by the transmitters, followed by a phase shift applied to the frequency-domain signal based on the information provided by the receiver.

<sup>1</sup>The blocks differing from conventional interleaved-ISAC (CI-ISAC) in the proposed PS-ISAC method are highlighted in blue.

<sup>2</sup>Since sensing sequences incorporate known pilot symbols for channel estimation, both sensing and communication transmitters can be treated similarly at the receiver. Thus, they are collectively referred to as transmitters, and both pilot and sensing sequences are simply termed pilots [11].

<sup>3</sup>Boldface lowercase symbols represent vectors.

Subsequently, the time-domain OFDM symbol is generated as

$$x_{T,u}^{ts}(n) = \frac{1}{\sqrt{N}} \sum_{k=0}^{N-1} x_{F,u}^{ps}(k) e^{j2\pi kn/N}, \quad n=0, 1, \dots, N-1, \quad (1)$$

where  $N$  represents the fast Fourier transform (FFT) size, and  $x_{F,u}^{ps}(k)$  denotes the phase-shifted pilot in the frequency domain. Then, a CP of size  $N_{CP}$  is appended. The signal is then processed through digital-to-analog conversion and transmitted over the channel by each transmitter separately. While the same  $N_{CP}$  is used for both communication and sensing symbols, different values may be assigned, provided the maximum excess delay of the channel is less than  $N_{CP}$ .

At the ISAC receiver, the received signal comprises the summation of all transmitted signals. The reception process begins with analog-to-digital conversion, followed by CP removal, yielding the time-domain signal  $y_T$ . Subsequently, the received frequency-domain signal  $y_F$  can be expressed as

$$y_F(k) = \sum_{u=1}^U h_{F,u}(k) x_{F,u}^{ps}(k) + w_u(k), \quad k=0, 1, \dots, N-1, \quad (2)$$

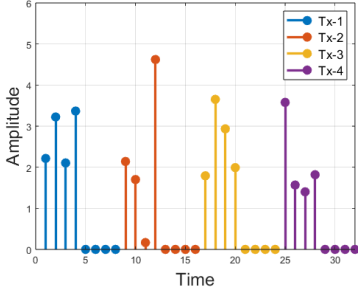
where  $h_{F,u}(k)$  represents the Rayleigh fading channel samples, modeled as  $\mathcal{CN}(0, 1)$ , and  $w_u(k)$  denotes an AWGN sample, modeled as  $\mathcal{CN}(0, \sigma^2)$ . After receiving the signal, channel estimation is performed, and the estimated channel frequency response (CFR) is subsequently transformed into the time domain via an inverse FFT (IFFT) operation for channel separation and noise cancellation [5]. The CIR of each transmitter is individually extracted in the time domain, followed by an FFT operation to recover the CFR for each transmitter. For parallel transmission, all communication and sensing transmitters are assumed to be perfectly synchronized with the receiver in both time and frequency domains.

## III. PROPOSED METHOD

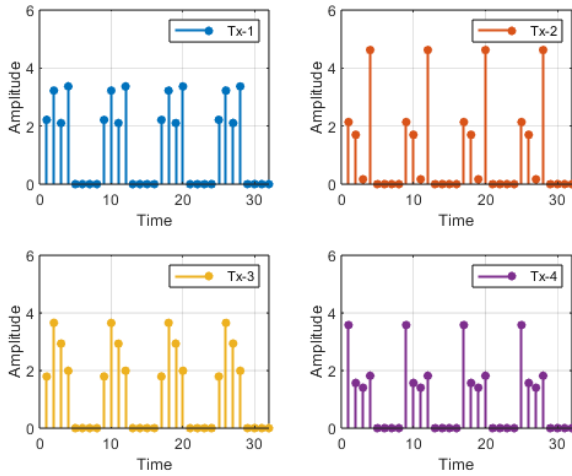
In CI-ISAC for OFDMA systems, pilots are utilized for both channel estimation and sensing [12], where the estimated channel is subsequently employed for either data demodulation or sensing tasks. However, in the proposed PS-ISAC, signals are fully overlapped in both the time and frequency domains, making conventional channel estimation infeasible due to

TABLE I  
COMPUTATIONAL COMPLEXITY OF CI-ISAC AND PS-ISAC.

	Transmitters		Receiver	
	CI-ISAC	PS-ISAC	CI-ISAC	PS-ISAC
Addition	$U(3N \log_2 N - 3N + 4)$	$U(3N \log_2 N - 3N + 4)$	$(2U + 1)(3N \log_2 N - 3N + 4)$	$(U + 2)(3N \log_2 N - 3N + 4)$
Multiplication	$U(N \log_2 N - 3N + 4)$	$U(N \log_2 N - N + 4)$	$(2U + 1)(N \log_2 N - 3N + 4) + 2N$	$(U + 2)(N \log_2 N - 3N + 4) + 2N$



(a) CIRs obtained using the PS-ISAC method.



(b) CIRs obtained using the CI-ISAC method.

Fig. 2. CIRs of transmitters at the receiver for different pilot design methods.

their inseparability. To address this limitation, phase-shifted pilot sequences are applied at the transmitters, allowing CIR separation at the receiver after the IFFT operation, where each transmitter's CIR appears at a distinct  $N_{CP}$  interval.

Prior to transmission, the receiver assigns each transmitter a phase shift based on  $N_{CP}$ , which is then applied to the pilot sequences in the frequency domain as

$$x_{F,u}^{ps}(k) = \psi_u(k)x_F(k), \quad (3)$$

where the phase shift introduces a corresponding time shift in the time domain after the IFFT operation. As illustrated in Fig. 1, each transmitter  $u$  applies the phase shift

$$\psi_u(k) = e^{-j2\pi kn_u/N}, \quad k = 0, 1, \dots, N-1, \quad (4)$$

where the phase shift amount is defined as  $n_u = (u-1)N_{CP}$ . Since  $N_{CP}$  is known at both the transmitter and receiver, no additional signaling overhead is required for timing synchronization. The only requirement is to transmit the assigned phase

shift to each transmitter, similar to the interleave subcarrier offset in conventional interleaved systems [16].

At the receiver, CFR estimation is performed using the known pilots  $\mathbf{x}_F$ . The received frequency-domain signal from (2) allows CFR estimation via the least-square (LS) estimator [5]. Unlike CI-ISAC, where LS is performed for each transmitter, in PS-ISAC, a single LS estimation is applied to all transmitters simultaneously. The estimated CFR is given by

$$\tilde{h}_F(k) = \frac{y_F(k)}{x_F(k)}, \quad k = 1, 2, \dots, N. \quad (5)$$

To enhance estimation accuracy, the estimated CFR is converted to CIR, facilitating multi-transmitter CIR separation as

$$\tilde{h}_T(n) = \frac{1}{\sqrt{N}} \sum_{k=0}^{N-1} \tilde{h}_F(k) e^{j2\pi kn/N}. \quad (6)$$

Then, transmitter-specific CFRs are extracted as

$$\tilde{h}_{F,u}(k) = \sqrt{N} \sum_{n=(u-1)N_{CP}}^{uN_{CP}-1} \tilde{h}_T(n) e^{-j2\pi nk/N}, \quad (7)$$

where the index selection in the FFT summation defines the CIR separation block, ensuring accurate differentiation of transmitter signals in the time domain, as shown in Fig. 1.

Fig. 2 illustrates the time-domain separation of transmitters' CIRs at the receiver, highlighting the distinction between the proposed PS-ISAC and CI-ISAC. The parameters used are  $N = 32$ ,  $U = 4$ ,  $N_{CP} = 8$ , a 4-tap frequency-selective Rayleigh fading channel, and pilot ratio (PR) =  $1/U$  with pseudo-random pilot sequences. In PS-ISAC, leveraging  $N_{CP}$  segments the received signal into intervals, enabling CIR separation in the time domain. Due to the overlapped block-pilot structure, periodicity does not appear in PS-ISAC. Conversely, CI-ISAC follows a fixed periodic structure, where interleaved pilots in the frequency domain introduce periodicity in time. This key difference allows PS-ISAC to separate CIRs in the time domain, whereas in CI-ISAC, CFR separation is achieved using transmitter-specific interleaved pilots.

#### A. Computational Complexity Analysis

The computational complexity analysis considers real additions (add.)/subtractions, multiplications (mult.)/divisions performed at the transmitter and receiver over an OFDM symbol duration. The FFT operation requires  $(3N \log_2 N - 3N + 4)$  real additions and  $(N \log_2 N - 3N + 4)$  real multiplications [17]. At the transmitters, IFFT complexity remains the same for both CI-ISAC and PS-ISAC, but PS-ISAC introduces additional overhead due to the phase shift operation, requiring  $2N$  real multiplications per transmitter. At the receiver, FFT complexities for both CI-ISAC and PS-ISAC are identical

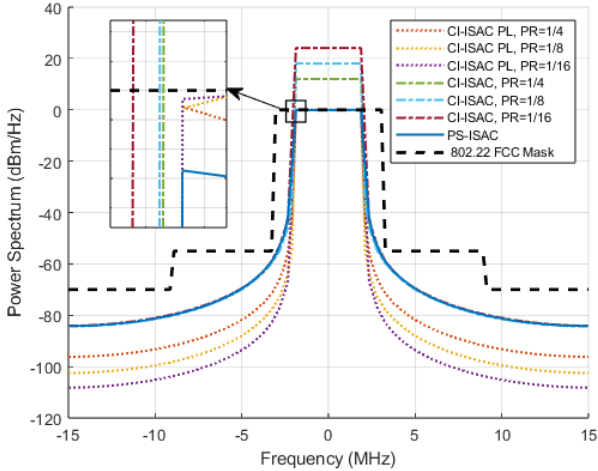


Fig. 3. Power spectra of CI-ISAC and PS-ISAC transmitters.

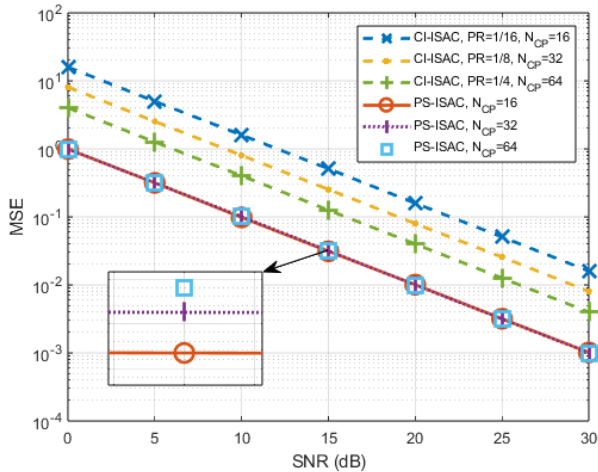


Fig. 4. MSE performance of CI-ISAC and PS-ISAC under power constraints.

when computing  $\mathbf{y}_F$  and  $\tilde{\mathbf{h}}_{F,u}$  in (7). Computing  $\mathbf{y}_F$  requires a single FFT for all transmitters, whereas obtaining  $\tilde{\mathbf{h}}_{F,u}$  requires an FFT for each transmitter. Both methods require  $2N$  real multiplications for  $\tilde{\mathbf{h}}_F$  estimation in (5). The key difference arises in IFFT operations at the receiver. In CI-ISAC, computing  $\tilde{\mathbf{h}}_{T,u}$  for each transmitter requires a separate IFFT, whereas in PS-ISAC, a single IFFT suffices, making it independent of the number of transmitters. A computational complexity comparison is provided in Table I.

### B. Maximum Unambiguous Range

The maximum unambiguous range is given by [13]

$$R_{\max} = \frac{N_p c}{2N \Delta f}, \quad (8)$$

where  $N_p$  is the number of pilot-carrying subcarriers,  $\Delta f$  is the subcarrier spacing, and  $c$  denotes the speed of light. In the interleaved structure,  $N_p$  is given by  $N_p = N \times \text{PR}$ , while in the proposed overlapped block-pilot method, it simplifies

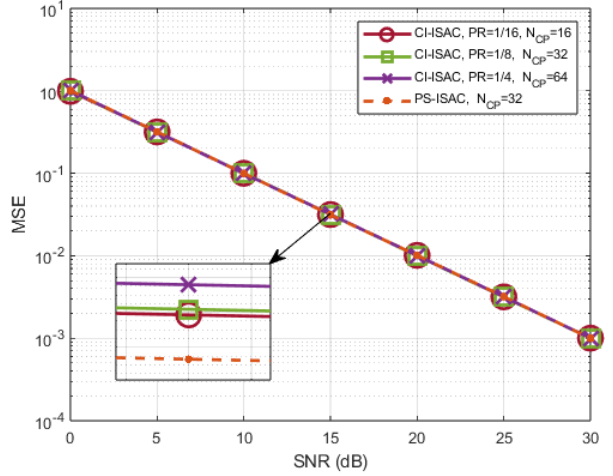


Fig. 5. MSE performance of CI-ISAC and PS-ISAC without power constraints.

to  $N_p = N$  since PR is set to 1. This confirms that the proposed method fully utilizes all available subcarriers for pilot allocation, achieving the theoretical limit for the maximum unambiguous range.

## IV. SIMULATION RESULTS

In this section, Monte Carlo simulations evaluate the MSE performance of PS-ISAC, alongside computational complexity and maximum unambiguous range analysis for a varying number of transmitters. The simulations use pseudo-random pilot sequences with  $N = 256$  and  $N_{CP} = N \times \text{PR}$ . Channels are modeled as  $(N_{CP} - 1)$ -tap frequency-selective Rayleigh fading, with  $U = 1/\text{PR}$ .

Fig. 3 examines the impact of power constraints (PC), comparing the PS-ISAC (PR = 1) with the CI-ISAC (PR = 1/4, 1/8, 1/16) under PC or without PC. In PC scenarios, each pilot subcarrier is normalized to unit power, while in non-PC cases, pilot subcarriers are scaled by  $\sqrt{1/\text{PR}}$  to maintain total power consistency with PR=1. However, as shown in Fig. 3, the non-PC approach exceeds the 802.22 FCC spectrum mask [18], while PS-ISAC and CI-ISAC under PC remain within the mask due to uniform power distribution across pilot carriers.

Figs. 4 and 5 compare MSE performances of PS-ISAC and CI-ISAC in PC and non-PC scenarios for different PR and  $N_{CP}$  values. The MSE is computed as  $\frac{1}{U} \sum_{u=1}^U \mathbb{E}[(\mathbf{h}_{F,u} - \tilde{\mathbf{h}}_{F,u})^2]$ . PS-ISAC achieves superior or comparable MSE performance to CI-ISAC, depending on the application of power constraints. Fig. 4 examines PS-ISAC under regulatory PC, showing consistent superiority over CI-ISAC across all PRs. Since PS-ISAC allows all transmitters to fully utilize subcarriers (PR=1), MSE remains independent of the number of transmitters. In contrast, CI-ISAC experiences degraded MSE as the number of transmitters increases relative to PR. The only trade-off in PS-ISAC is its higher pilot power usage per transmitter compared to CI-ISAC. Fig. 5 illustrates the MSE performance without PC, showing that PS-ISAC achieves the same MSE as CI-ISAC. Since the MSE remains unchanged

TABLE II  
COMPUTATIONAL COMPLEXITY COMPARISON BETWEEN CI-ISAC AND PS-ISAC.

Method	U	Transmitters		Receiver	
		Add.	Mult.	Add.	Mult.
CI-ISAC	4	21520	5136	48420	12068
	8	43040	10272	91460	22340
	16	86080	20544	177540	42884
PS-ISAC	4	21520	7184	32280	8216
	8	43040	14368	53800	13352
	16	86080	28736	96840	23624

TABLE III  
MAXIMUM UNAMBIGUOUS RANGE COMPARISON BETWEEN CI-ISAC AND PS-ISAC.

Method	U	$R_{\max}(\text{m})$
CI-ISAC	4	2498
	8	1249
	16	624
PS-ISAC	4/8/16	9993

for any  $N_{\text{CP}}$  value due to the overlapped block-pilot allocation, only  $N_{\text{CP}} = 32$  is presented for PS-ISAC.

The computational complexity calculations for a varying number of transmitters are summarized in Table II. Results show that PS-ISAC consistently has lower computational complexity than CI-ISAC, with the difference becoming more significant as the number of transmitters increases. This is due to PS-ISAC requiring only a single IFFT at the receiver for CIR estimation. While transmitter complexity is slightly higher due to the phase shift operation, it remains negligible compared to the computational cost of IFFT, especially for large values of  $N$ .

Table III highlights the maximum unambiguous range advantage of PS-ISAC. When  $\text{PR}=1$ , the proposed method achieves the highest possible  $R_{\max}$ , whereas in CI-ISAC,  $R_{\max}$  decreases as the number of transmitters increases. Overall, PS-ISAC not only maximizes the maximum unambiguous range with significantly lower computational complexity but also achieves superior MSE performance under power constraints while maintaining equivalent MSE when power constraints are not applied. These results underscore the efficiency of PS-ISAC in resource-constrained environments.

## V. CONCLUSION

This paper proposes a novel overlapped block-pilot allocation method for uplink OFDMA-based ISAC systems, leveraging a CP-based phase-shifted pilot design to enable the separation of the CIRs from multiple transmitters at the receiver. Theoretical analysis and simulations confirm that PS-ISAC substantially reduces computational complexity by eliminating the need for transmitter-specific IFFT operations at the receiver, compared to the CI-ISAC method. Additionally, it maintains the highest achievable maximum unambiguous range and enhances the MSE performance under power constraints. These advantages make PS-ISAC as a scalable and efficient pilot design solution for next-generation ISAC networks.

## REFERENCES

- [1] Liu, F., Cui, Y., Masouros, C., Xu, J., Han, T. X., Eldar, Y. C., and Buzzi, S., "Integrated sensing and communications: Toward dual-functional wireless networks for 6G and beyond," *IEEE J. Sel. Areas Commun.*, vol. 40, no. 6, pp. 1728–1767, 2022.
- [2] Liu, Y., Huang, T., Liu, F., Ma, D., Huangfu, W., and Eldar, Y. C., "Next-generation multiple access for integrated sensing and communications," *Proc. IEEE*, 2024.
- [3] Tusha, A., and Arslan, H., "Interference Burden in Wireless Communications: A Comprehensive Survey from PHY Layer Perspective," *IEEE Commun. Surveys Tuts.*, 2024.
- [4] Liu, Y., Zhang, S., Mu, X., Ding, Z., Schober, R., Al-Dhahir, N., Hossain, E., and Shen, X., "Evolution of NOMA toward next generation multiple access (NGMA) for 6G," *IEEE J. Sel. Areas Commun.*, vol. 40, no. 4, pp. 1037–1071, 2022.
- [5] Ozdemir, M., and Arslan, H., "Channel estimation for wireless OFDM systems," *IEEE Commun. Surveys Tuts.*, vol. 9, no. 2, 2007.
- [6] Wei, Z., Wang, Y., Ma, L., Yang, S., Feng, Z., Pan, C., Zhang, Q., Wang, Y., Wu, H., and Zhang, P., "5G PRS-Based Sensing: A Sensing Reference Signal Approach for Joint Sensing and Communication System," *IEEE Trans. Veh. Technol.*, vol. 72, no. 3, pp. 3250–3263, 2023.
- [7] Du, R., Hua, H., Xie, H., Song, X., Lyu, Z., Hu, M., Narengerile, Xin, Y., McCann, S., Montemurro, M., Han, T. X., and Xu, J., "An Overview on IEEE 802.11bf: WLAN Sensing," *IEEE Commun. Surveys Tuts.*, vol. 27, no. 1, pp. 184–217, 2025.
- [8] Yaacoub, E., and Dawy, Z., "A Survey on Uplink Resource Allocation in OFDMA Wireless Networks," *IEEE Commun. Surveys Tuts.*, vol. 14, no. 2, pp. 322–337, 2012.
- [9] Ribeiro, C. M., Fernández-Getino García, M. J., Gil Jiménez, V. P., Gameiro, A., and García Armada, A., "Uplink Channel Estimation for Multi-user OFDM-based Systems," *Wireless Pers. Commun.*, vol. 47, pp. 125–136, 2008.
- [10] Sternad, M., and Aronsson, D., "Channel estimation and prediction for adaptive OFDMA/TDMA uplinks, based on overlapping pilots," *Proc. IEEE Int. Conf. Acoust. Speech Sig. Process.*, vol. 3, pp. 861–864, 2005.
- [11] Ozkaptan, C. D., Ekici, E., Altintas, O., and Wang, C.-H., "OFDM Pilot-Based Radar for Joint Vehicular Communication and Radar Systems," *IEEE Veh. Netw. Conf.*, pp. 1–8, 2018.
- [12] Wang, C.-H., Altintas, O., Ozkaptan, C. D., and Ekici, E., "Multi-Range Joint Automotive Radar and Communication using Pilot-based OFDM Radar," *IEEE Veh. Netw. Conf.*, pp. 1–4, 2020.
- [13] Mei, D., Wei, Z., Chen, X., Wang, L., and Feng, Z., "A Coprime and Periodic Pilot Design for ISAC System," *IEEE Wireless Commun. and Netw. Conf.*, pp. 1–6, 2024.
- [14] Memisoglu, E., Türkmen, H., Ozbakis, B. A., and Arslan, H., "CSI-based NOMA for integrated sensing and communication," *IEEE Wireless Commun. Lett.*, vol. 12, no. 6, pp. 1086–1090, 2023.
- [15] Demir, A. B., Memisoglu, E., and Arslan, H., "CSI-based Sensing with NOMA of Multiple Sensing Users for ISAC," *IEEE Globecom Workshops*, pp. 1398–1403, 2023.
- [16] 3GPP, "NR; Physical Channels and Modulation," *3rd Generation Partnership Project (3GPP), Technical Report 38.211*, January 2025.
- [17] Sorensen, H. V., Heideman, M., and Burrus, C., "On computing the split-radix FFT," *IEEE Trans. Acoust., Speech, and Signal Process.*, vol. 34, no. 1, pp. 152–156, Feb. 1986.
- [18] Tom, A., Sahin, A., and Arslan, H., "Mask compliant precoder for OFDM spectrum shaping," *IEEE Commun. Lett.*, vol. 17, no. 3, pp. 447–450, 2013.